Rational design and fabrication of multiphasic soft network composites for tissue engineering articular cartilage: A numerical model-based approach

Onur Bas[a,b,f], Sara Lucarotti[a,c], Davide D. Angella[d,e], Nathan J. Castro[a,f], Christoph Meinert[a,f], Felix M. Wunner[a], Ernst Rank[d,e], Giovanni Vozzi[c], Travis J. Klein[b,f], Isabelle Catelas[f,g], Elena M. De-Juan-Pardo[a,f], Dietmar W. Hutmacher[a,b,d,f,*]

[a] *Centre in Regenerative Medicine, Institute of Health and Biomedical Innovation, Queensland University of Technology (QUT), Kelvin Grove, Brisbane, QLD 4059,*

Australia

[b] *ARC Training Centre in Additive Biomanufacturing, Queensland University of Technology (QUT), Brisbane, QLD 4059, Australia*

[c] *Research Center "E. Piaggio", University of Pisa, 56100 Pisa, Italy*

[d] *Institute for Advanced Study, Technische Universität München, D-85748 Garching, Germany*

[e] *Chair for Computation in Engineering, Technische Universität München, D-80333 Munich, Germany*

[f] *School of Chemistry, Physics and Mechanical Engineering, Science and Engineering Faculty, Queensland University of Technology (QUT), Brisbane, QLD 4001, Australia*

[g] *Department of Mechanical Engineering, University of Ottawa, Ottawa, ON, K1N 6N5, Canada*

∗ Corresponding author at: ARC Training Centre in Additive Biomanufacturing, Queensland University of Technology (QUT), Brisbane, QLD 4059, Australia.

E-mail address: dietmar.hutmacher@qut.edu.au (D.W. Hutmacher).

Keywords:

Soft network composites; Melt electrospinning writing; Articular cartilage; Rational design; Gelatin methacryloyl; Multiphasic; 3D printing; Soft tissue engineering; Fibers

Abstract

There is an urgent need in the field of soft tissue engineering (STE) to develop biomaterials exhibiting a high degree of biological and mechanical functionality as well as modularity so that they can be tailored according to patient-specific requirements. Recently, biomimetic soft network composites (SNC) consisting of a water-swollen hydrogel matriX and a reinforcing fibrous network fabricated by melt electrospinning writing technology have demonstrated exceptional mechanical and biological properties, thus becoming strong candidates for STE ap- plications. However, there is a lack of design approaches to tailor and optimize their properties in a non-empirical way. To address this challenge, we propose a numerical model-based approach for the rational design of patient-specific SNC for tissue engineering applications. The approach is rooted in an in silico design library that allows for the selection of biomaterial and architecture combinations for the target application, resulting in reduced time, manpower and costs. To demonstrate the validity of the design strategy, a multiphasic SNC with predefined zone-specific properties that captured the complex zonal mechanical and compositional features of articular cartilage was developed based on the natural design of the native tissue.

1. Introduction

The development of biomaterials with a high level of both biological and mechanical functionality addressing the intricate requirements of soft tissue engineering (STE) applications is an ongoing challenge. One approach is to develop new biomaterials that meet these requirements by including particular biological motifs into a structurally appropriate polymer. Alternatively, well-characterized single phase biomaterials with a proven performance for a desired function can be combined into multi-functional composites via advanced manufacturing technologies and rational design strategies. Composite systems with design-centric constituents can leverage the advantages of each material and lead to unique, sometimes unexpected, properties suited for specific applications. Examples can be found in a wide range of areas, and may appear as a simple straw-reinforced mud-brick or a high-performance aero- space material [1–3]. Materials of natural origin, with almost no exception, also show a composite design [4]. In the case of soft biological materials, composite structures in the form of fiber-reinforced biopolymer gels resembling soft network composites (SNC) are commonly observed. The potential of this particular composite design for STE applications has been recognized, and thus, an increasing number of studies aim towards the development of its tissue-engineered analogues.

The most promising composite designs for such STE applications are probably the ones that consist of a water-swollen hydrogel matrix and a reinforcing fibrous network made of a biodegradable polymer [5–8]. In these composites, similarly to soft biological materials, the hydrogel matrix provides a suitable microenvironment for cells to function, and the high-modulus fibers are primarily responsible for providing a structural integrity and strength. We have also shown in previous studies that the combination of fibrous networks fabricated by melt electrospinning writing (MEW), a technology utilizing additive manufacturing and electrospinning principles [9], with soft hydrogels results in SNC with enhanced biological and mechanical functionality [10–12]. Owing to the capabilities of MEW and the applicability of the established reinforcement concept to a wide range of hydrogel types, the design and composition of the SNC presented in these previous studies can readily be tailored for patient- and tissue-specific applications. This versatility is critically important for such composite systems as each tissue engineering (TE) application may require an SNC exhibiting different mechanical, biological and physicochemical properties. However, this flexibility could turn into one of the main challenges for the design process of SNC with customized set of properties, as there are countless potential combinations of materials and fiber architectures available. To explicitly meet the design objectives via conventional development approaches in such multi-variant systems, a significant number of iterations is often required for the design, fabrication and characterization until the desired properties are achieved [13]. One promising approach to address this challenge is to bring the emerging concept of rational design utilizing computational models into play [14–16]. Such computationally-guided biomaterials design strategies have been shown to be highly favorable for complex design problems where multiple design variables have to be taken into account [17,18]. Recently, we developed a numerical model that employs high order finite element modelling (*p*-FEM) to investigate the deformation characteristics of particular SNC designs for which results were in good accordance with the experimental findings [19]. Similarly to this particular study, a great number of numerical models are found in the literature to simulate and study the behavior of complex biological or synthetic systems [20–24]. Yet, the scope of their application is rarely extended to the rational design phase for the development of composite biomaterials.

In the present study, we propose an original numerical model-based approach for the rational design of SNC as substitutes of complex bio- logical materials (Fig. 1a). To do so, a design library that allows predicting the compressive modulus of SNC (E_{SNC}) was established using hydrogel matrix and the reinforcing fibers), and the compressive numerical tools (Fig. 1b). The design library consists of 500 different simulated SNC models and allows for the derivation of ESNC from the compressive modulus (E_{MatriX}) and Poisson's ratio (v_{MatriX}) of a hydrogel matriX of interest. The model facilitates the selection of suitable net- work designs (pore size and fiber diameter) for a given hydrogel matriX and fiber material to obtain a SNC with a desired compressive modulus. The library was specifically developed for soft hydrogel matrices (E_{MatriX} ranging from 10 to 50 kPa), which display suitable mechanical properties for encapsulation of various cell types such as human

chondrocytes [25], human umbilical vein endothelial cells [26] and mesenchymal stem cells [27], as well as for reinforcing meshes exhibiting a cross-shaped 0°–90° fiber lay-down pattern.

To demonstrate the validity of the presented design strategy, a multiphasic SNC with predefined zonal mechanical properties was developed, rooted in the natural design of articular cartilage. In a previous study, we have shown that material selection and design strategies following the blueprints of the native tissue lead to SNC that match the overall transient, equilibrium and viscoelastic properties of knee articular cartilage [19]. Yet, the mechanical properties of articular cartilage are known to vary for each patient and with the location of the tissue [28], which requires customization for improved mechanical conformity of the engineered constructs to the corresponding defect site location. Moreover, articular cartilage is a bio-composite characterized by a multiphasic structure that comprises three distinct zones, namely superficial, middle and deep, each distinguished by their different compositional, structural and mechanical characteristics [29,30]. So far, the exquisite zonal mechanical and compositional features of the tissue from nano- to micro- to macro-scale have not been considered in the design of SNC consisting of highly organized micrometer-size fibers and a biomimetic hydrogel matriX. Therefore, articular cartilage, an ongoing clinical challenge, was selected to demonstrate the validity of our rational design approach. Photo-crosslinkable methacryloyl functionalized gelatin (GelMA) was chosen for the matriX due to its good biocompatibility, inherently available integrin cell-binding and pro- tease-cleavage motifs, and tunable mechanical properties [31]. Medical grade poly(ε-caprolactone) (mPCL) was chosen for the reinforcing fibrous network, due to its excellent processability via MEW and proven performance in vitro and in vivo, in addition to its clinical track record in FDA-approved and CE-marked devices [32,33].

2. Experimental

2.1 Numerical model and in silico design library

p-version of the finite element method (*p*-FEM) was implemented in the numerical model due to its low computational cost when simulating elements with high aspect ratios [34]. The reinforcing fibers in the SNC exhibit a very high aspect ratio, which makes *p*-FEM a suitable methodology for the study of SNC. In the standard numerical modelling methodology (*h*-FEM) that is employed in the majority of commercially available software, the number of the mesh elements is increased to improve the accuracy of the numerical solution. Although this approach is very effective to solve a wide range of engineering problems, it re- quires assignment of large numbers of mesh elements while simulating geometries consisting of features with a high aspect ratio. This leads to increased computational costs [35]. In contrast, *p*-FEM increases the number of the polynomial degree of the elements rather than the number of elements for improved accuracy, and is generally computationally cost-effective and faster for such geometries [35]. The details of the structure and design of the numerical model are beyond the scope of this article and are described elsewhere [19]. Briefly, hexahedral elements were used to describe the geometry of the SNC. A linear elastic material model was assigned for both constituents of the system (the hydrogel matrix and the reinforcing fibers), and the compressive modulus (E) and Poisson's ratio (v) values were assigned for each mesh element describing each material. Each section of the fibers was de- scribed as an extruded body of an octagon. The elements filling the void between the fibers were used to model the hydrogel matriX. Symmetry conditions were applied to further reduce the computational cost of the simulations, where one quarter of each construct was simulated, which numerically describes the entire geometry. ESNC values of the simulated SNC were derived by using the internal energy extrapolation method [36]. Internal energy values obtained from simulations performed at polynomial degrees of 4, 6 and 8 were used for the extrapolation.

Five hundred (500) different design frameworks were batch-processed using the numerical model to generate the data for the virtual library. The diameter range of the fibers of the reinforcing networks examined was between approXimately 5 and 25 μm. The fibers in this diameter range provide a high surface-

area-to-volume ratio and enable reasonably high-throughput fabrication of clinically-relevant size constructs in a reproducible manner via MEW. The virtual library generated was supported with theoretically calculated volumetric hydrogel fraction data of the resultant SNC, which is an important criterion for biomaterials design (Fig. 1d).

2.2 Fabrication of fibrous networks

An in-house built MEW device was used to print the fibrous net- works [37]. Briefly, mPCL pellets (Purasorb® PC 12, Corbion Purac, The Netherlands) were melted in a 3cc plastic syringe using two heaters. The temperatures of heater #1 (placed near the syringe) and heater #2 (placed near the needle) were set to 75 °C and 85 °C, respectively. The molten polymer was extruded through a 23G needle using an electro-pneumatic pressure regulator (ITV1050, SMC, Japan) at different air pressures (0.25, 0.50, 1.0, 1.5, 2.0, 2.5 and 3.0 bars). A high voltage of 7–10 kV was applied to the needle to form an electrified jet that accelerates towards the grounded collector. Different translational speeds of the collector were used (between 500 mm/min and 2500 mm/min) for the printing process. The printing settings were modified to be able to obtain fibers with different diameters (between ∼5 and 25 μm) (Table 1 and Fig. 1b). Forty (40) mm X 40 mm fibrous networks with a fiber lay-down pattern of 0°–90° were printed in a layer-by-layer manner until a height of 1.8 mm was reached. For the fabrication of the multiphasic SNC, the MEW device was paused after printing 10 layers of mPCL/hydroXyapatite nanoparticles (nHA) composite fibers, and the material in the syringe was exchanged to mPCL before resuming the print.

Table 1 Parameters used to obtain fibers with a diameter of 5, 10, 15, 20 or 25 μm using MEW (n = 6 for fiber diameter measurements).

Fiber diameter (μm)		Applied pressure (bars)	Translational collector speed (mm/min)	Applied voltage (kV)	Temperature (°C)	
Target	Printed				Heater 1	Heater 2
5	4.8 ± 0.3	0.25	2500	7.2	75	85
10	10.4 ± 0.2	0.5	1000	7	75	85
15	15.3 ± 0.8	2	1250	10	75	85
20	20.2 ± 0.4	2.5	1000	9.3	75	85
25	24.6 ± 0.7	3	750	9	75	85

2.3 Fabrication of soft network composites

A custom-made injection molding system made of polytetrafluoroethylene (PTFE; Teflon®) and consisting of wells having a 5.0 mm diameter and 1.8 mm height was used for the preparation of the SNC. Circular fibrous network cuts (5.0 mm diameter) were obtained from the printed meshes (40.0 mm × 40.0 mm) using a laser cutter, as de- scribed elsewhere [6]. The circular fibrous network cuts were placed into the wells of the PTFE mold. GelMA from porcine skin-derived gelatin (Gelita, Australia) was prepared with a functionalization degree of 70%, following a previously described protocol [31]. In the present study, a photo-initiator, lithium acylphosphinate (LAP) [38] exciting at a visible light wavelength (405 nm), was used for the polymerization of GelMA pre-gel instead of an ultraviolet (UV) light-initiated crosslinking system that has been associated with several safety risks. LAP con- centration of 0.15% (w/v) was used to provide a good crosslinking in a short period of time and a reproducible manner. GelMA (10% (w/v)) with a high degree of methacrylation exhibits a high stability and relatively low mass swelling properties making it a suitable matrix material to validate our design methodology [26,39]. The wells were filled with the pre-gel solution of GelMA with LAP, closed with a glass-slide, and photo-crosslinked at different durations (10 s, 30 s, 1 min, 2.5 min, 5 min and

10 min). The samples were allowed to swell for 24–36 h in Dulbecco's Modified Eagle medium (DMEM) (Sigma Aldrich, USA) at 37 °C before further characterization.

2.4. Imaging and µCT analysis

Scanning electron microscopy (SEM) images shown in Figs. 2 and 4 were captured using a FEI Quanta 200 (FEI, Netherlands) and a TM3000 Hitachi (Hitachi, Japan) microscope, respectively. An image processing software, ImageJ (National Instruments, USA), was used to measure the diameter of the fibers on the micrographs (n = 6, three measurements on two different micrographs). Stereomicroscopy imaging was performed using a Nikon SMZ 745T microscope (Nikon Instruments Inc., Japan).

Micro-computational tomography (µCT) analysis was performed using a Scanco mCT40 scanner (Scanco Medical AG, Switzerland) at a voltage of 45 kVp, a current of 177 mA, an integration time of 300 ms, and an averaging of 6. VoXel size of 6 µm was used during the scans.

2.5. Mechanical characterization

Mechanical properties of the SNC were tested under uniaxial com- pression loading in an unconfined arrangement between non-porous platens at a displacement rate of 0.01 mm/s using an Instron MicroTester equipped with a 5N load cell (Instron, Australia). To simulate the physiological conditions, the samples were submerged in pre-warmed cell medium (DMEM at 37 °C) during the testing. The slope of the strain-stress curves (between strains of 0.10 and 0.15) was used to derive the compressive moduli (ESNC) of the tested specimens. During the compression tests, images of the tested hydrogels were captured to be able to track the dimensional changes in response to the applied strain (0.30). The images were then used to calculate the Poisson's ratios (ratios of lateral strains to axial strains). Unless otherwise stated, all data are expressed as mean values ± standard deviations (n = 5 for mechanical tests).

3. Results and discussion

To test the prediction capability of the design library that was created, SNC designs selected from the library were fabricated and mechanically characterized, and the values obtained from these physical tests were compared to those generated from their simulated counter- parts. Two systematic comparison studies were performed. For the first benchmarking, fibrous networks with a fiber diameter of 15 µm and pore sizes of 200, 400, 600 and 800 µm were fabricated to be combined with a hydrogel (see Fig. 2a for MEW fibers with different line spacing). This fiber diameter was in the middle of the investigated diameter range (5–25 µm) in the simulations. For the second experiment, fibrous networks with a pore size of 400 µm and fiber diameters of 5, 10, 15, 20 and 25 µm were fabricated. First, a systematic study was performed to be able to identify the settings for the in-house built MEW device for printing fibers within the aforementioned fiber diameter range (Fig. 2b and c). The findings are shown in Fig. 2b, and the exact values used for printing fibers with diameters of 5, 10, 15, 20 and 25 µm are summarized in Table 1.

E of 30 kPa was targeted for the hydrogel matriX of the tested SNC, which is the middle value of the examined range in the library (10–50 kPa). A pilot study was performed to identify the light exposure time that yields hydrogels with E of 30 kPa. To do so, casted GelMA pre- gel solutions were exposed to the light for different durations (10 s, 30 s, 1 min, 2.5 min, 5 min and 10 min), and their E values were subsequently measured. The

obtained values were curve-fitted using two- phase association equation (GraphPad Prism 7, GraphPad Software, Inc., USA) (R2 = 0.961), and based on the constructed mathematical function, a light exposure time of 37 s was determined to be required to reach E of 30 kPa (Fig. 3a).

Next, the printed fibrous networks were used to reinforce the GelMA hydrogel, and the resulting SNC were mechanically characterized. First, the mechanical properties of the GelMA were investigated to confirm that the desired EMatriX value was reached. Light exposure of 37 s on 10% (w/v) GelMA + 0.15% (w/v) LAP yielded a hydrogel with EMatriX of 30.60 ± 4.11 kPa, which met the targeted E value (30 kPa). Poisson's ratio (v) of this hydrogel was found to be 0.484 ± 0.015 when it was compressed at a displacement rate of 0.01 mm/s. Such high v was expected since the hydrogel matriX is primarily composed of water, which is considered as an incompressible material. Subsequently, the mechanical tests were performed on the fabricated SNC. E values of the tested SNC were compared to those of their simulated counterparts that exhibited the closest properties (see Fig. 3b and c for the simulation and experimental SNC parameters). Although slightly lower E values were obtained in the experiments in comparison to those obtained via simulations for SNC reinforced with thin fibers (diameters of 5 and 10 µm), pairwise comparisons showed a good match in the majority of the E values (7 out of 9 test conditions) (Fig. 3b and c). The relatively low values measured in the physical experiments can be attributed to the challenges in fabricating fibrous networks with very fine fibers while maintaining good manufacturing tolerances. This increased the differences between the geometries of the physically fabricated SNC and their simulated perfect counterparts. Nevertheless, the findings suggest that the design library has good prediction cap- abilities, in particular for SNC consisting of reinforcing fibers with diameters larger than 15 µm. It is expected that the minor discrepancy between the simulation and experimental results could be reduced or completely removed by enhancing the technological capabilities of MEW hardware to improve the deposition accuracy of the fibers at lower length scales.

Besides using the model as a prediction tool, the data generated in silico allowed for the precise investigation of the influence of each de- sign variable, providing substantial insights into the mechanical prop- erties of SNC. Based on the findings from the simulations, ESNC increases with increasing EMatriX, vMatriX, EFiber, fiber diameter and decreasing pore size (Fig. 3b–f). The relation between ESNC and EMatriX, EFiber or the fiber diameter was found to be relatively linear within the investigated parameter ranges. However, vMatriX led to significant increases in ESNC when it was increased from 0.450 to 0.495.

It is known that the zonal mechanical differences in articular cartilage are highly associated with the variations in the organization and density of the collagen network [40]. With that in mind, a SNC consisting of a structurally-graded fibrous network was fabricated to obtain a stiffness gradient in the SNC comparable to that of articular cartilage (see Fig. 4a for the schematic illustration of the translated design concept). For the hydrogel matriX, E of 40 kPa was selected to allow fabricating SNC with E comparable to that of the native tissue. Based on the findings presented in Fig. 3a, pre-gel solutions were exposed to light for 62 s, which yielded hydrogels with E of 39.84 ± 3.80 kPa. Pore size and fiber diameter of the reinforcing networks were regionally modified in the SNC with the guidance of the design library (see Table 2 for the specifications of the hypothetical multiphasic SNC design for articular cartilage repair). Moreover, articular cartilage exhibits a partial mineralization at the region that connects the tissue to the underlying subchondral bone. MEW technology has successfully been implemented to 3D-print composite fibers with nanoparticles for bone TE applications [41,42]. Emulation of the calcified zone of articular cartilage by using nanometer-size inorganic particles embedded in microfibers may improve the regenerative outcome of SNC. Therefore, 10 layers of mPCL/nHA composite fibers (5% (w/w) of nanoparticle content) mimicking the mineralized collagens were printed at the bottom of the fibrous network of the SNC.

As the 3D reconstructions from µCT images and SEM micrographs of the fibrous networks in Fig. 4b and c demonstrate, MEW was proven to be highly versatile and allowed the fabrication of multiphasic fibrous network designs consisting of highly ordered microfibers with pre-de- fined fiber diameters. The dispersion of nHA nanoparticles in melt electrospun mPCL fibers was found uniform with the size of the aggregates

being generally less than 1 μm on the SEM micrographs (Fig. 4d). These minor aggregate formations were not detectable on the μCT images (Fig. 4b).

The ability of MEW to fabricate intricate designs with microfibers, its additive manufacturing integration and its solvent-free processing characteristics distinguish MEW from other fiber processing techniques such as solution electrospinning, knitting, weaving and braiding. These capabilities allowed for the translation of intended designs into physical fibrous networks with good manufacturing tolerances. Hydrogels were then infiltrated into the pores of the printed fibrous networks to fabricate multiphasic SNC. A representative stereomicroscopy image of the resulting SNC is shown in Fig. 4e. The mechanical tests performed for each zone showed that the targeted ESNC values were slightly lower than anticipated while the simulated ESNC values fell between the experimental error bounds (Table 2).

It is essential to note that several assumptions were made while performing the simulations. First, the materials were assumed to be fully isotropic and flawless, and the imposed contacts and boundary conditions were idealized. Moreover, a linear elastic material model was used to describe both of the composite constituents and could only partly capture their behavior. For instance, SNC presented in this work exhibit strong time- and strain rate-dependent mechanical properties [11,19], but the material model that was used was not capable of capturing these behaviors. Therefore, all simulations were performed in steady-state conditions based on the test results performed at a specific strain rate. Yet, the findings from the simulations presented in this work were in line with those obtained from the physical tests and allowed for predicting ESNC at a low computational cost. The capabilities of the design library can be further advanced with material models that take into account the dynamic interplays between the interstitial fluid and solid constituents. For example, material models based on biphasic [43] and poroelastic [44] theories have been employed to predict time- and strain rate-dependent mechanical behavior of articular cartilage, and may be applied to describe the hydrogel matriX of SNC. An important criteria when designing biomaterials for articular cartilage regeneration is the frictional properties of the resulting tissue-engineered construct. Systematic investigations of the design parameter and the incorporation of its relationship with the stiffness of SNC into the design library could further advance the capabilities of the presented design methodology. The result is a comprehensive in silico design library. Also, by investigating the degradation kinetics of the materials used and the in- fluence of extracellular matriX development, it may be possible to set better initial design criteria (e.g., baseline values for ESNC and factor of safety parameter) for SNC to prevent their premature failure after im- plantation. Moreover, this library could be further extended using data sets generated from in vitro studies conducted with high-throughput combinatorial screening methods in order to provide predictions from not only biomechanical but also molecular and cell biology-related properties of the resultant SNC.

Table 2 Specifications of multiphasic soft network composite (SNC) design intended to capture the gradients in the compressive moduli of articular cartilage. The properties of designed SNC and those of fabricated SNC are compared (n = 5 for physically fabricated SNC).

	Targeted E_{SNC} (kPa)	SNC design output from the library				Fabricated E_{SNC}	
		*E*Matrix (kPa)	Pore size (μm)	Fiber diameter (μm)	E_{SNC} (kPa)	*E*Matrix (kPa)	E_{SNC} (kPa)
Superficial zone	500	40	800	25	569.1	39.8 ± 3.8	491.7 ± 103.0
Transitional zone	1500	40	400	25	1552.7	39.8 ± 3.8	1340.4 ± 143.7
Deep zone	2500	40	200	20	2660.5	39.8 ± 3.8	2425.8 ± 574.6

4. Conclusion

In the present study, a design strategy based on a numerical model was applied to accelerate the design of specific SNC for applications in TE and regenerative medicine. An in silico design library was established to guide the biomaterial scientist and/or bioengineer to select the most promising SNC designs for a STE application in order to minimize time, cost and efforts dedicated to fabrication and experimental testing. A case study was performed for articular cartilage as a proof of concept. The model allowed the prediction of the most biomechanically-suited SNC designs to reflect multiphasic zonal features of articular cartilage. The multiphasic SNC was combined with a mPCL/nHA architecture to mimic the cartilage calcified zone. Further in vitro and in vivo studies have to validate that the biomechanical conformity and biomimetic material composition of the engineered SNC positively affect the re- generative potential of engineered articular cartilage.

Acknowledgements

The authors thank Prof. Hans G. Börner and Dr. FeliX Hansske (both Humboldt-Universität zu Berlin) for providing mPCL/nHA composites, and Dr. Christoph Lahr for his assistance in µCT scanning. This work was financially supported by the ARC Centre in Additive Biomanufacturing and assisted by the Hans Fischer Senior Fellowship at the Institute for Advanced Study, Technische Universität München.

References

[1] K.K. Chawla, Carbon Fiber/Carbon MatriX Composites BT - Composite Materials: Science and Engineering, Springer New York, New York, NY, 2012, pp. 293–307, http://dx.doi.org/10.1007/F978-0-387-74365-3_8.

[2] D. Gay, Composite Materials : Design and Applications, 3rd ed., CRC Press, Bosa Roca, 2014.

[3] S. Ramakrishna, J. Mayer, E. Wintermantel, K.W. Leong, Biomedical applications of polymer-composite materials: a review, Compos. Sci. Technol. 61 (2001) 1189–1224, http://dx.doi.org/10.1016/S0266-3538(00)00241-4.

[4] Z. Liu, M.A. Meyers, Z. Zhang, R.O. Ritchie, Functional gradients and hetero- geneities in biological materials: design principles, functions, and bioinspired ap- plications, Prog. Mater. Sci. 88 (2017) 467–498, http://dx.doi.org/10.1016/j. pmatsci.2017.04.013.

[5] L.A. Bosworth, L.A. Turner, S.H. Cartmell, State of the art composites comprising electrospun fibres coupled with hydrogels: a review, nanomedicine nano- technology, Biol. Med. 9 (2013) 322–335, http://dx.doi.org/10.1016/j.nano.2012. 10.008.

[6] A.L. Butcher, G.S. Offeddu, M.L. Oyen, Nanofibrous hydrogel composites as me- chanically robust tissue engineering scaffolds, Trends Biotechnol. 32 (2014) 564–570, http://dx.doi.org/10.1016/j.tibtech.2014.09.001.

[7] S. Xu, L. Deng, J. Zhang, L. Yin, A. Dong, Composites of electrospun-fibers and hydrogels: a potential solution to current challenges in biological and biomedical field, J. Biomed. Mater. Res. – Part B Appl. Biomater. 104 (2016) 640–656, http:// dx.doi.org/10.1002/jbm.b.33420.

[8] D. Puppi, C. Migone, L. Grassi, A. Pirosa, G. Maisetta, G. Batoni, F. Chiellini, Integrated three-dimensional fiber/hydrogel biphasic scaffolds for periodontal bone tissue engineering, Polym. Int. 65 (2016) 631–640, http://dx.doi.org/10.1002/pi. 5101.

[9] T.D. Brown, P.D. Dalton, D.W. Hutmacher, Direct Writing By Way of Melt Electrospinning, Adv. Mater. 23 (2011) 5651–5657, http://dx.doi.org/10.1002/ adma.201103482.

[10] J. Visser, F.P.W. Melchels, J.E. Jeon, E.M. van Bussel, L.S. Kimpton, H.M. Byrne,

W.J.A. Dhert, P.D. Dalton, D.W. Hutmacher, J. Malda, Reinforcement of hydrogels using three-dimensionally printed microfibres, Nat. Commun. 6 (2015) 6933, http://dx.doi.org/10.1038/ncomms7933.

[11] O. Bas, E.M. De-Juan-Pardo, M.P. Chhaya, F.M. Wunner, J.E. Jeon, T.J. Klein, D.W. Hutmacher, Enhancing structural integrity of hydrogels by using highly or- ganised melt electrospun fibre constructs, Eur. Polym. J. 72 (2015) 451–463, http://dx.doi.org/10.1016/j.eurpolymj.2015.07.034.

[12] O. Bas, D. D'Angella, J.G. Baldwin, N.J. Castro, F.M. Wunner, N.T. Saidy, S. Kollmannsberger, A. Reali, E. Rank, E.M. De-Juan-Pardo, D.W. Hutmacher, An integrated design, material and fabrication platform for engineering biomechani- cally and biologically functional soft tissues, ACS Appl. Mater. Interfaces (2017) 29430–29437, http://dx.doi.org/10.1021/acsami.7b08617.

[13] G. Hautier, A. Jain, S.P. Ong, From the computer to the laboratory: materials dis- covery and design using first-principles calculations, J. Mater. Sci. 47 (2012) 7317–7340, http://dx.doi.org/10.1007/s10853-012-6424-0.

[14] A.A. Zadpoor, Biomaterials and tissue biomechanics: a match made in heaven? Materials (Basel). 10 (2017) 528, http://dx.doi.org/10.3390/ma10050528.

[15] M.E. Eberhart, D.P. Clougherty, Looking for design in materials design, Nat. Mater. 3 (2004) 659–661, http://dx.doi.org/10.1038/nmat1229.

[16] J. Kohn, T. Road, New approaches to biomaterials design, Nat. Mater. 3 (2004) 745–747, http://dx.doi.org/10.1038/nmat1249.

[17] M.J. Mirzaali, R. Hedayati, P. Vena, L. Vergani, M. Strano, A.A. Zadpoor, Rational design of soft mechanical metamaterials: independent tailoring of elastic properties with randomness, Appl. Phys. Lett. 111 (2017) 51903, http://dx.doi.org/10.1063/ 1.4989441.

[18] S.J. Hollister, C.Y. Lin, Computational design of tissue engineering scaffolds, Comput. Methods Appl. Mech. Eng. 196 (2007) 2991–2998, http://dx.doi.org/10. 1016/j.cma.2006.09.023.

[19] O. Bas, E.M. De-Juan-Pardo, C. Meinert, D. D'Angella, J.G. Baldwin, L.J. Bray, R.M. Wellard, S. Kollmannsberger, E. Rank, C. Werner, T.J. Klein, I. Catelas, D.W. Hutmacher, Biofabricated soft network composites for cartilage tissue en- gineering, Biofabrication 9 (2017) 25014 http://stacks.iop.org/1758-5090/9/i=2/ a=025014.

[20] J.F.M. Ribeiro, S.M. Oliveira, J.L. Alves, A.J. Pedro, R.L. Reis, E.M. Fernandes, J.F. Mano, Structural monitoring and modeling of the mechanical deformation of three-dimensional printed poly(ε -caprolactone) scaffolds, Biofabrication 9 (2017) 25015, http://dx.doi.org/10.1088/1758-5090/aa698e.

[21] A. Alberich-Bayarri, D. Moratal, J.L. Escobar Ivirico, J.C. Rodriguez Hernandez, A. Valles-Lluch, L. Marti-Bonmati, J.M. Estelles, J.F. Mano, M.M. Pradas, J.L. Gomez Ribelles, M. Salmeron-Sanchez, Microcomputed tomography and microfinite ele- ment modeling for evaluating polymer scaffolds architecture and their mechanical properties, J. Biomed. Mater. Res. – Part B Appl. Biomater 91 (2009) 191–202, http://dx.doi.org/10.1002/jbm.b.31389.

[22] J.L. Milan, J.A. Planell, D. LacroiX, Computational modelling of the mechanical environment of osteogenesis within a polylactic acid-calcium phosphate glass scaffold, Biomaterials 30 (2009) 4219–4226, http://dx.doi.org/10.1016/j. biomaterials.2009.04.026.

[23] A. Vahdati, D.R. Wagner, Finite element study of a tissue-engineered cartilage transplant in human tibiofemoral joint, Comput. Methods Biomech. Biomed. Eng. 15 (2012) 1211–1221, http://dx.doi.org/10.1080/10255842.2011.585974.

[24] P. Julkunen, W. Wilson, H. Isaksson, J.S. Jurvelin, W. Herzog, R.K. Korhonen, A review of the combination of experimental measurements and fibril-reinforced modeling for investigation of articular cartilage and chondrocyte response to loading, Comput. Math. Methods Med. 2013 (2013), http://dx.doi.org/10.1155/ 2013/326150.

[25] P.A. Levett, D.W. Hutmacher, J. Malda, T.J. Klein, Hyaluronic acid enhances the mechanical properties of tissue-engineered cartilage constructs, PLoS One. 9 (2014) e113216, http://dx.doi.org/10.1371/journal.pone.0113216.

[26] J.W. Nichol, S.T. Koshy, H. Bae, C.M. Hwang, S. Yamanlar, A. Khademhosseini, Cell-laden microengineered gelatin methacrylate hydrogels, Biomaterials 31 (2010) 5536–5544, http://dx.doi.org/10.1016/j.biomaterials.2010.03.064.

[27] O. Chaudhuri, L. Gu, D. Klumpers, M. Darnell, S.A. Bencherif, J.C. Weaver, N. Huebsch, H. Lee, E. Lippens, G.N. Duda, D.J. Mooney, Hydrogels with tunable stress relaxation regulate stem cell fate and activity, Nat. Mater. 15 (2016) 326–334, http://dx.doi.org/10.1038/nmat4489.

[28] V.C. Mow, X.E. Guo, Mechano-electrochemical properties of articular cartilage: their inhomogeneities and anisotropies, Annu. Rev. Biomed. Eng. 4 (2002) 175–209, http://dx.doi.org/10.1146/annurev.bioeng.4.110701.120309.

[29] M. Wong, D.R. Carter, Articular cartilage functional histomorphology and me- chanobiology: a research perspective, Bone 33 (2003) 1–13, http://dx.doi.org/10. 1016/S8756-3282(03)00083-8.

[30] J. Becerra, J.A. Andrades, E. Guerado, P. Zamora-Navas, J.M. López-Puertas, A.H. Reddi, Articular cartilage: structure and regeneration, Tissue Eng. Part B Rev. 16 (2010) 617–627, http://dx.doi.org/10.1089/ten.teb.2010.0191.

[31] D. Loessner, C. Meinert, E. Kaemmerer, L.C. Martine, K. Yue, P.A. Levett, T.J. Klein, F.P.W. Melchels, A. Khademhosseini, D.W. Hutmacher, Functionalization, pre- paration and use of cell-laden gelatin methacryloyl-based hydrogels as modular tissue culture platforms, Nat. Protoc. 11 (2016) 727–746, http://dx.doi.org/10. 1038/nprot.2016.037.

[32] S.M. Young, G. Sundar, T.-C. Lim, S.S. Lang, G. Thomas, S. Amrith, Use of bior- esorbable implants for orbital fracture reconstruction, Br. J. Ophthalmol. 101 (2017) 1080–1085, http://dx.doi.org/10.1136/bjophthalmol-2016-309330.

[33] M.A. Woodruff, D.W. Hutmacher, The return of a forgotten polymer—Polycaprolactone in the 21st century, Prog. Polym. Sci. 35 (2010) 1217–1256, http://dx.doi.org/10.1016/j.progpolymsci.2010.04.002.

[34] E. Rank, A. Düster, V. Nübel, K. Preusch, O.T. Bruhns, High order finite elements for shells, Comput. Methods Appl. Mech. Eng. 194 (2005) 2494–2512, http://dx.doi. org/10.1016/j.cma.2004.07.042.

[35] B. Szabó, A. Düster, E. Rank, The p-Version of the Finite Element Method, Encycl. Comput. Mech, John Wiley & Sons, Ltd, 2004, pp. 119–139, , http://dx.doi.org/10. 1002/0470091355.ecm003g.

[36] B. Szabó, I. Babuška, Generalized Formulations, Introd. to Finite Elem. Anal. John Wiley & Sons, Ltd, 2011, pp. 109–144, , http://dx.doi.org/10.1002/ 9781119993834.ch4.

[37] F.M. Wunner, O. Bas, N.T. Saidy, P.D. Dalton, E.M.D. Pardo, D.W. Hutmacher, Melt electrospinning writing of three-dimensional poly (ε-caprolactone) scaffolds with controllable morphologies for tissue engineering applications, J. Vis. EXp. (2017) 1–12, http://dx.doi.org/10.3791/56289.

[38] B.D. Fairbanks, M.P. Schwartz, C.N. Bowman, K.S. Anseth, Photoinitiated poly- merization of PEG-diacrylate with lithium phenyl-2,4,6-trimethylbenzoylpho- sphinate: polymerization rate and cytocompatibility, Biomaterials 30 (2009) 6702–6707, http://dx.doi.org/10.1016/j.biomaterials.2009.08.055.

[39] W. Schuurman, P.A. Levett, M.W. Pot, P.R. van Weeren, W.J.A. Dhert, D.W. Hutmacher, F.P.W. Melchels, T.J. Klein, J. Malda, Gelatin-methacrylamide hydrogels as potential biomaterials for fabrication of tissue-engineered cartilage constructs, Macromol. Biosci. 13 (2013) 551–561, http://dx.doi.org/10.1002/ mabi.201200471.

[40] J.S. Jurvelin, M.D. Buschmann, E.B. Hunziker, Mechanical anisotropy of the human knee articular cartilage in compression, Proc. Inst. Mech. Eng. Part H J. Eng. Med. 217 (2003) 215–219, http://dx.doi.org/10.1243/095441103765212712.

[41] X. Qu, P. Xia, J. He, D. Li, Microscale electrohydrodynamic printing of biomimetic PCL/nHA composite scaffolds for bone tissue engineering, Mater. Lett. 185 (2016) 554–557, http://dx.doi.org/10.1016/j.matlet.2016.09.035.

[42] F. Hansske, O. Bas, C. Vaquette, G. Hochleitner, J. Groll, E. Kemnitz, D. Hutmacher, H. Boerner, Via precise interface engineering towards bioinspired composites with improved 3D printing processability and mechanical properties, J. Mater. Chem. B. (2017) 5037–5047, http://dx.doi.org/10.1039/C7TB00165G.

[43] V.C. Mow, S.C. Kuei, W.M. Lai, C.G. Armstrong, Biphasic creep and stress relaxation of articular cartilage in compression? Theory and experiments, J. Biomech. Eng. 102 (1980) 73–84, http://dx.doi.org/10.1115/1.3138202.

[44] M.A. Biot, General theory of three-dimensional consolidation, J. Appl. Phys. 12 (1941) 155–164, http://dx.doi.org/10.1063/1.1712886.

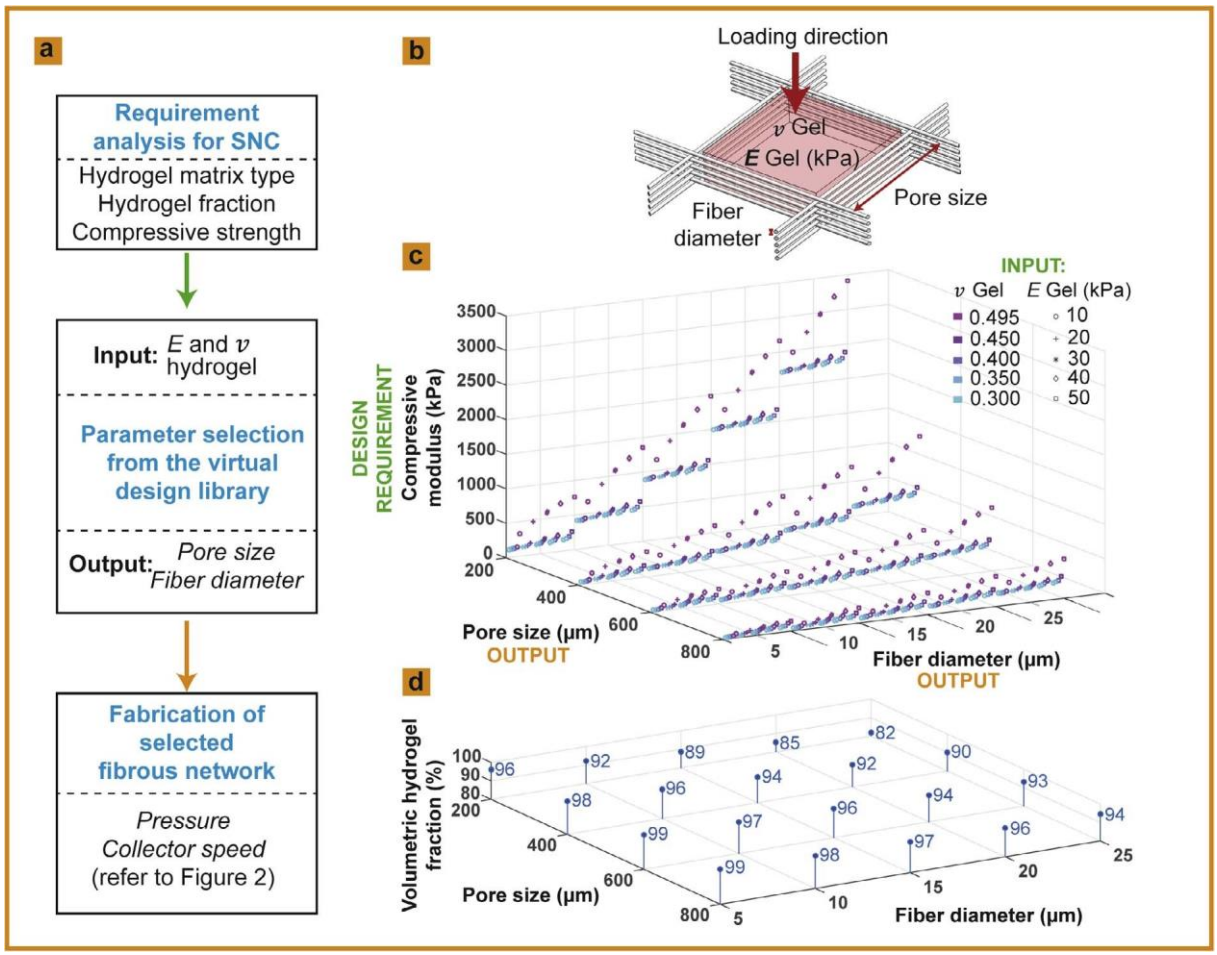

Figure 1. a) A numerical model-based design strategy applied for soft network composites. b) Schematic illustration of a unit cell of a soft network composite (SNC) with design variables. c–d) The library developed for the rational design of patient-specific SNC for articular cartilage repair. The library allows for the estimation of c) the compressive modulus (E), and is supported with d) the volumetric hydrogel fraction values of different SNC combinations. The simulations were performed for medical grade poly(ε-caprolactone) (mPCL) fibers (EmPCL = 317.18 MPa and vmPCL = 0.3 were used as the input values to define mPCL fibers [19]).

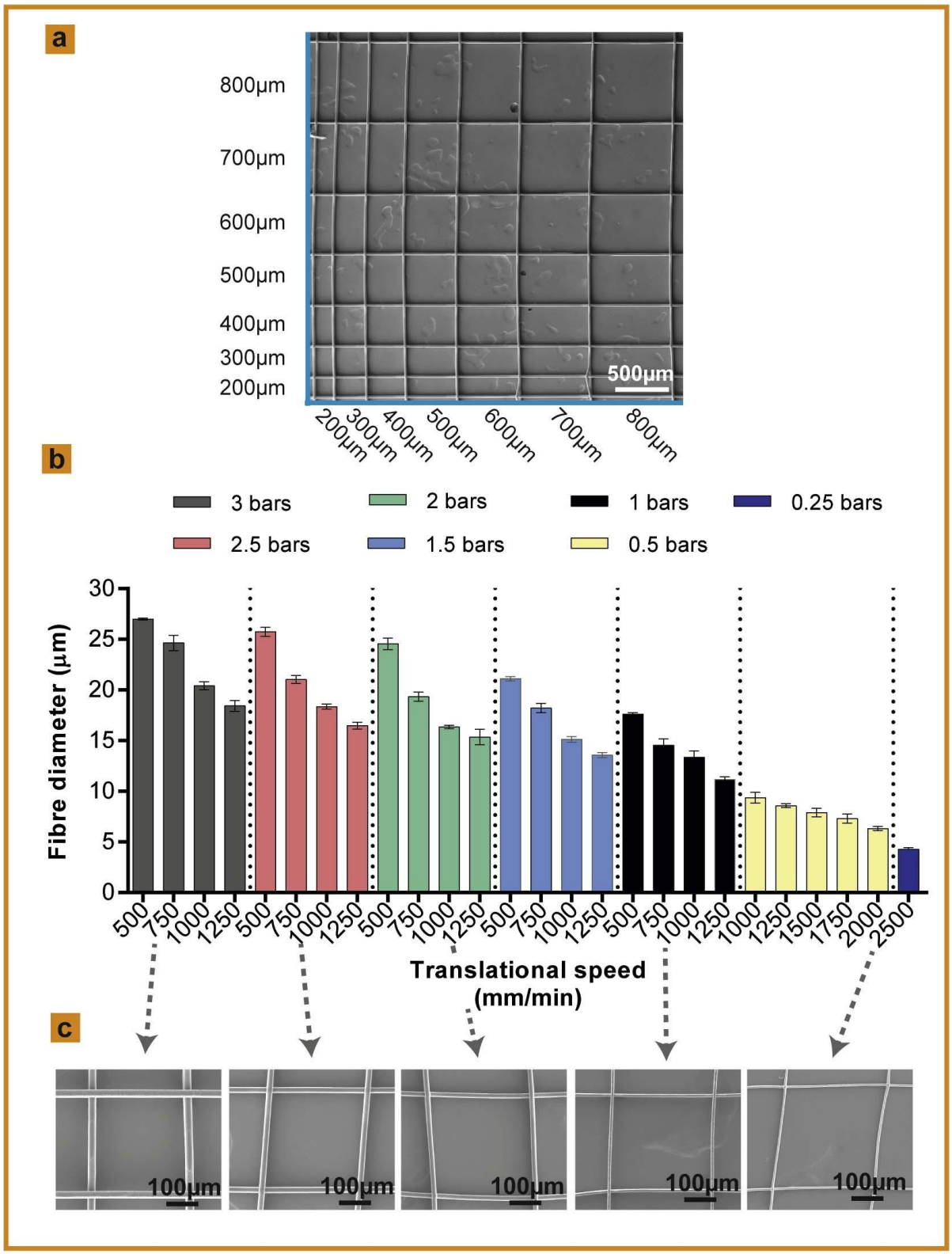

Figure 2. a) Fibers printed with different pore sizes demonstrating the capabilities of melt electrospinning writing (MEW) technology. b) Graph showing the influence of the translational collector speed and applied pressure on the fiber diameter (n = 6 measurements for each condition illustrated in Fig. 2b) with c) representative scanning electron microscopy (SEM) images.

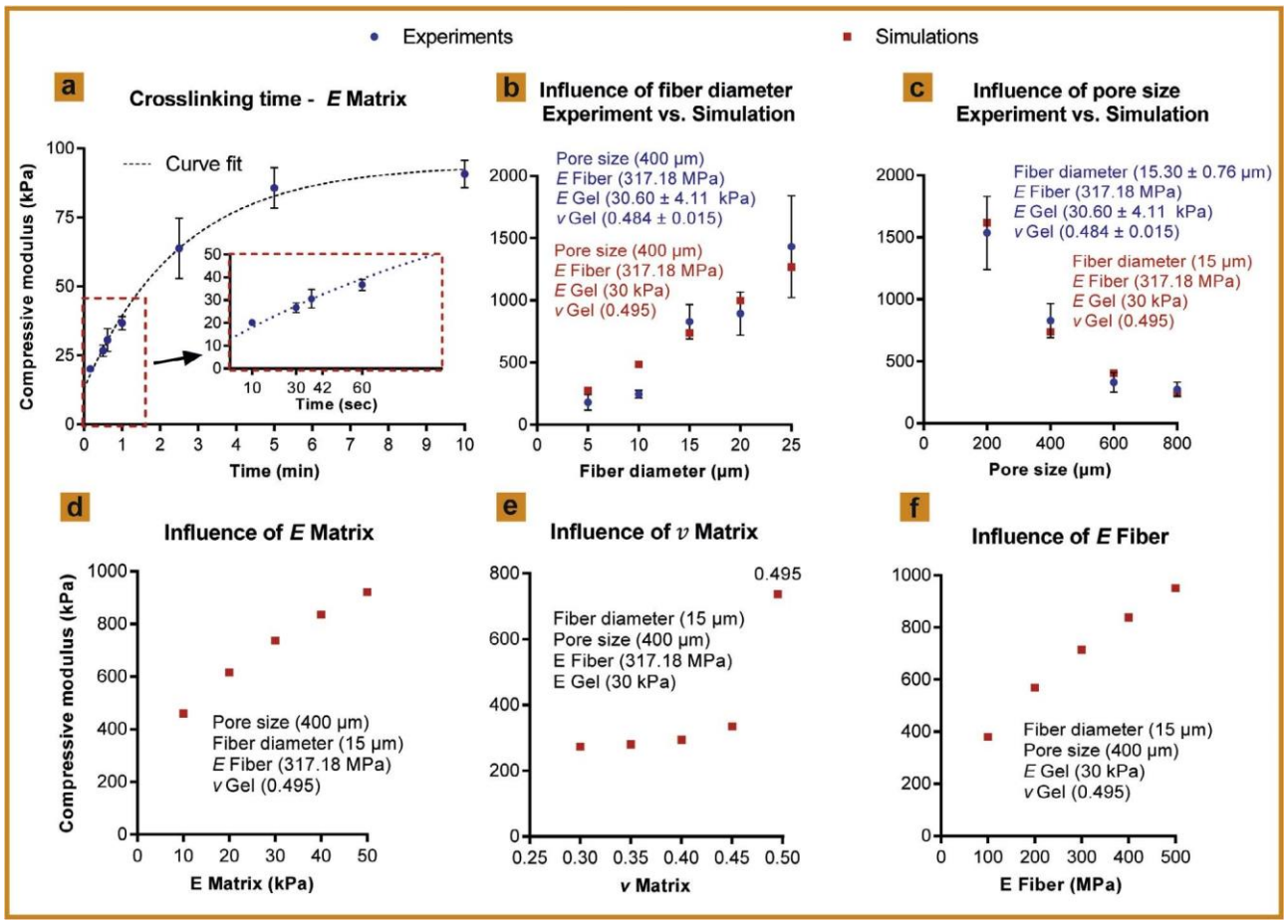

Figure 3. a) Influence of light exposure time on the compressive modulus (E) of GelMA hydrogel (10% w/v) with LAP (0.15% (w/v)). b–f) Influence of hydrogel matriX (EMatriX and vMatriX) and fibrous network (fiber diameter, pore size and EFiber) properties on the E of the resultant soft network composites (SNC). The values were taken from the design library to plot the figures (red color), and were used to investigate the influence of each design variable. All simulations were performed for mPCL fibers except (f), where polymers with different E values were explored. b–c) Comparison of the simulation results with those obtained from physical experiments to test the prediction capabilities of the design library (n = 5 for the experimental test values in Fig. 3a–c).

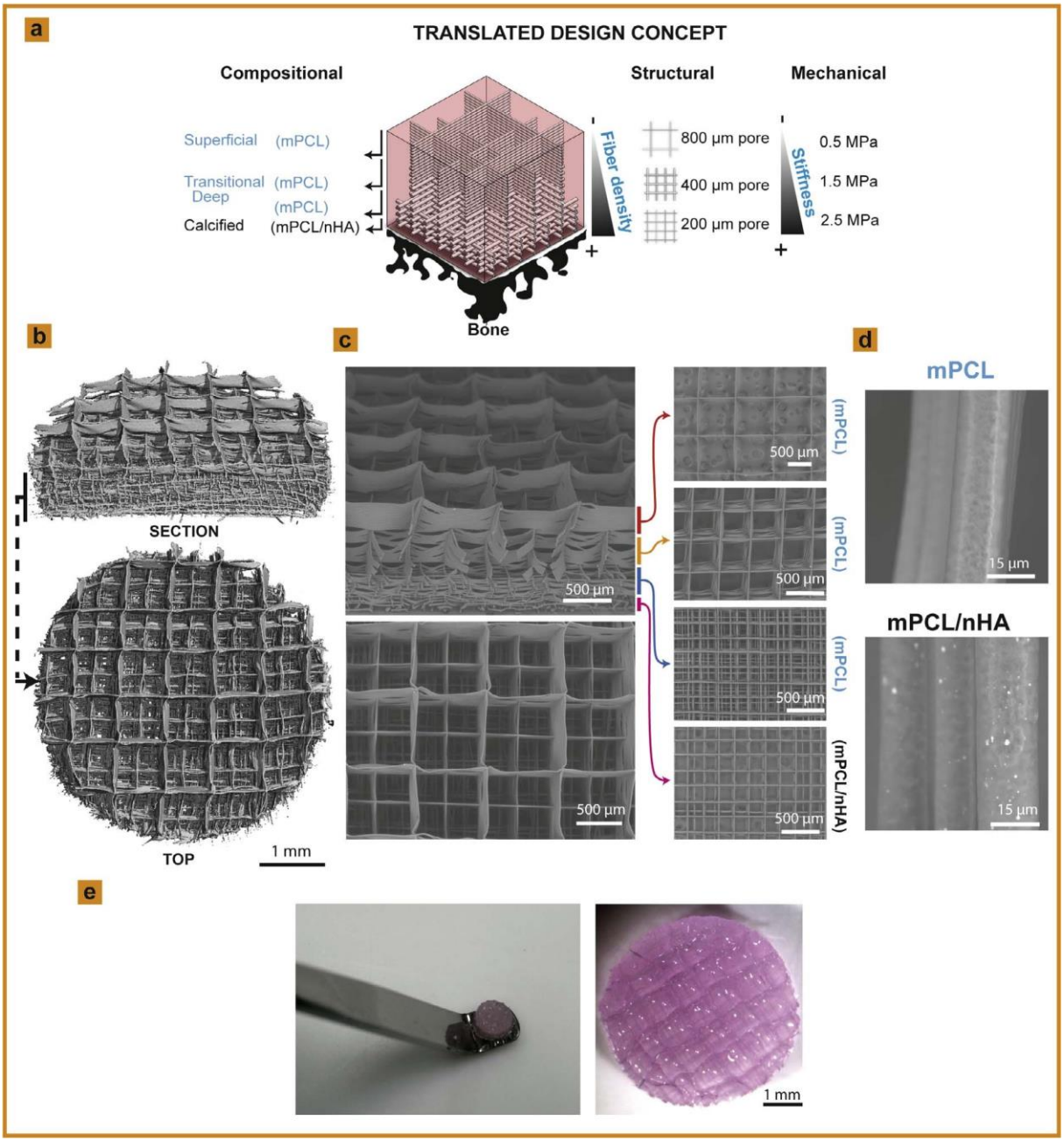

Figure 4. a) Design concept translating compositional, functional and biomechanical features of native articular cartilage into soft network composites (SNC). Mechanical properties of non- mineralized superficial, translational and deep zones of articular cartilage were captured using structurally graded medical grade poly(ε-caprolactone) (mPCL) fibers. Fiber diameter and pore size of the fibrous networks were determined a priori using the design library. Composite fibers composed of mPCL and hydroXyapatite nanoparticles (nHA) (mPCL/5% (w/w) nHA) were used to emulate the calcified zone of the tissue. b) 3D-µCT reconstruction and c) Scanning electron microscopy (SEM) images of the multiphasic fibrous network printed via melt electrospinning writing (MEW) with individual zones. d) SEM images of mPCL and composite fibers. e) Images of a representative SNC.